Scientia Iranica (2024) 31(20), 1880-1888

Sharif University of Technology

Scientia Iranica

Transactions B: Mechanical Engineering

https://scientiairanica.sharif.edu

Modeling of jet electrochemical machining using numerical and design of experiments methods

Ali Mehrvar *, Mohsen Motamedi, and Abouzar Jamalpour

Department of Mechanical Engineering, Shahreza Campus, University of Isfahan, Isfahan, Iran.

* Corresponding author: a.mehrvar@shr.ui.ac.ir (A. Mehrvar)

Received 27 March 2022; received in revised form 20 July 2023; accepted 15 October 2023

Keywords

Jet electrochemical machining;
Modeling;
Finite element method;
Design of experiments;
Optimization.

Abstract

Modeling and determining the optimal conditions for the Jet Electrochemical Machining (Jet-ECM) process is critical. In this study, a hybrid approach combining numerical and Design of Experiments (DOE) methods have been applied to model and determine the optimal conditions for Jet-ECM. The voltage (V), inner tool diameter (I), initial machining gap (G), and electrolyte conductivity (C) are considered input variables. Additionally, dimensional accuracy (E) and machining depth (D) are response variables. Twenty-seven numerical simulations have been performed using the Box–Behnken design to implement the Response Surface Methodology (RSM). Consequently, two mathematical models have been obtained for these response variables. The effects of the input variables on the response variables are investigated using statistical techniques such as variance analysis. Furthermore, the desirability function approach has been applied to determine the optimal conditions for dimensional accuracy and depth of machining. The results show that the optimal values for achieving maximum depth of machining while maintaining a dimensional accuracy of 0.05 mm are as follows: electrolyte conductivity of 8 S/m, voltage of 36.9 V, initial machining gap of 200 μm, and inner tool diameter of 0.4 mm.

1. Introduction

Electrochemical Machining (ECM) is one of the most economical and efficient methods in modern subtractive manufacturing processes. This machining process involves anodic dissolution, following Faraday's relationship [1]. Importantly, there is no contact between the cathode and the anode; thus, there is no stress on the part's surface. Furthermore, the hardness and toughness of the workpiece do not affect the machining process, and the tool does not wear out [2-4]. One variant of ECM is Jet Electrochemical Machining (Jet-ECM), which employs a nozzle-shaped tool to jet the electrolyte into the space between the tool and the workpiece [5].

The fundamental principle of Jet-ECM is anodic dissolution. In this process, the nozzle is connected to the negative pole, while the workpiece is connected to the positive pole of the power supply. The space between them is filled with an electrolyte jet, and the machining occurs by Faraday's law [6]. Jet-ECM finds applications in drilling, grooving, reducing surface roughness, and creating texture, especially in small dimensions [7-9].

Although the jet concept was initially introduced in machining in the 1980s [10], recent years have witnessed intensified research and development regarding functional capabilities and process simulation [11]. However, modeling and developing this machining process pose challenges due to various physical, chemical, and hydrodynamic phenomena. Additionally, numerous factors and parameters influence the utilization of the process [12-15]. On the other hand, effectively applying this process to different materials and applications necessitates costly and time-consuming experimentation and trial and error. Hence, this study presents an approach that combines numerical analysis and the Design of Experiments (DOE) method to model, determine optimal conditions, and investigate the effect of process parameters on machining performance. Initially, existing research in Jet-ECM simulation and application is reviewed, followed by developing the proposed approach for process investigation.

This work proposes a 3D Finite Element Method (FEM) simulation model for channel machining using Scanning Micro Electrochemical Flow Cell (SMEFC) and Jet-ECM [16]. The FEM model is based on Faraday's law, a virtual thin electrolyte layer, and a moving mesh technique. Notably, the simulation enables the movement of electrolyte droplets over a relatively large range on the workpiece. The model concurrently

To cite this article:

A. Mehrvar, M. Motamedi, and A. Jamalpour "Modeling of jet electrochemical machining using numerical and design of experiments methods", *Scientia Iranica* (2024), **31**(20), pp. 1880–1888. https://doi.org/10.24200/sci.2023.60185.6650

determines the current density and potential distribution while altering the workpiece profile, thus enhancing the understanding of this type of ECM process [16]. Another study presents a multi-physical model for Jet-ECM simulation using COMSOL Multiphysics [17]. The simulation results are compared and validated with experimental and previous simulation results, which employ a static jet shape. This simulation considers fluid dynamics and an electrical resistance boundary at the interface between the workpiece and the electrolyte [17]. Additionally, a three-dimensional finite volume model for Jet-ECM simulation is presented in this paper [18].

The multi-physical model was created using the commercial software STAR-CCM+. This model includes fluid dynamics regarding the two-phase flow of the electrolyte and the air. Based on the normal electric current density calculated on the workpiece surface, machining is modeled according to Faraday's law using geometric deformation [18].

The Jet-ECM of Ti-6Al-4V has been investigated with the help of ultrasonic in this paper [19]. Using ultrasonic increased the aspect ratio of the grooves and the depth and decreased the kerf. On the other hand, according to the frequency selected in this study, the formation of the inactive layer was reduced to 23% [19]. In another research, the Jet-ECM for polishing and patterning of LPBF Ti-6Al-4V components has been investigated [20]. The results of this research were the reduction of surface roughness and the creation of a datum surface [20].

Furthermore, a numerical and experimental investigation of Jet-ECM with the help of inclined nozzles was studied by Liu et al. [21]. With an inclined nozzle, the flow velocity distribution and the thickness of the electrolyte layer around the jet are uneven. Thus, an asymmetric hydraulic jump and anodic current density distribution is created. In addition, the effects of the nozzle inclined angle and electrolyte outflow velocity were investigated. In another study, the creation of multi-grooves by Jet-ECM was done by Luo et al. with the help of simulation and experimental investigation [22]. In creating multiple grooves simultaneously, if the tubes are too close, the electrolyte jets interfere, seriously affecting the performance of multiple grooves, such as reducing machining accuracy and stray corrosion in unnecessary areas. This simulation and experimental investigation showed that the appropriate distance between the tubes and their insulation increased accuracy (reduced stray corrosion) [22]. Moreover, simulations have been performed in this research due to the importance of a jet's shape in Jet-ECM [23]. According to the Jet-ECM process, the simulation is divided into two steps. In the first step, the jet is formed. In the second step, the anodic dissolution is simulated to determine the deformation of the workpiece. In another study, the masked Jet-ECM of a micro through-slit array on a thin metal plate was investigated by Chen et al. [24]. A mathematical model was developed for this process and used to simulate the machining of a micro through-slit array.

Moreover, the Jet-ECM with a continuous electrolyte jet is being investigated as a potential method for machining tungsten carbide alloys [25]. The effects of input parameters, such as the type of electrolyte and voltage, and output parameters, like aspect ratio and surface roughness, were investigated [25]. Another study examined the effect of the gas and electrolyte mixture in Jet-ECM for creating holes and grooves [26]. This mixture increases the current density, thereby increasing the Material Removal Rate (MRR) and the efficiency of the process. Conversely, low current density leads to stray corrosion and reduced surface quality, which should be avoided [26].

Additionally, micro dimples, used as a surface texture to enhance performance and efficiency, were investigated by Chen et al. [27]. To address the need for minimizing additional machining and improving the location of micro dimples, the process involves directly applying a conductive patterned mask to the workpiece. This approach eliminates the requirement for an insulated patterned mask and reduces the necessity for extra machining.

Furthermore, the Jet-ECM process typically involves the vertical impact of the electrolytic jet downstream of the workpiece. As a result, other jet orientations, such as upward, vertical, and horizontal orientations, are rarely utilized. In this study, three jet directions were implemented for Jet-ECM, and the impact of jet orientation on machining performance was investigated [28].

This research's primary contribution lies in applying a hybrid approach for process modeling and optimization in the Jet-ECM process. Specifically, the combination of Response Surface Methodology (RSM) and numerical methods, establishing sub-models, and optimization techniques were employed to determine process conditions and optimal solutions. No previous investigations have employed this approach for modeling and optimizing this process. Selecting optimal and suitable process parameters is crucial in manufacturing processes, particularly in the Jet-ECM process. Therefore, this research represents the first attempt to propose predefined optimal solutions, considering conflicting cost functions in this process, using the desirability function approach. In other words, the optimal condition for achieving maximum machining depth (MRR) was determined while ensuring dimensional accuracy does not exceed 0.05 mm. The proposed approach can be applied in various conditions of this process or other processes where conducting actual experiments is challenging due to limited materials and tools and complex modeling and predicting optimum process parameters.

2. Design of Experiment (DOE)

In the DOE, changes are consciously made to the input variables of the process to observe and identify the resulting changes in the output responses [29]. The process can be regarded as a combination of factors and parameters in the Jet-ECM to enhance machining performance. Machining performance is characterized by one or more response variables, such as MRR, accuracy, and surface quality. This study's response variables are the depth of machining (D) and dimensional accuracy (E).

Each input parameter was evaluated at three levels. The input parameters include machining voltage (V) in volts, electrolyte conductivity (C) in Siemens per meter (S/m), initial machining gap (G) in μm, and nozzle inside diameter (I) in μm. The DOE method employed in this research is the RSM, utilizing the Box-Behnken design and Minitab software. Consequently, the input parameters and their levels are presented in Table 1. The number of simulations conducted in the COMSOL software totaled 27. The remaining fixed parameters for the modeling process are listed in Table 2.

Table 1. Input parameters and their levels [22,24,26,27].

Machining Parameter	Symbol	Level (–1)	Level (0)	Level (1)
Electrolyte conductivity	C (S/m)	8	12	16
Initial machining gap	G (μm)	200	350	500
Voltage	V (Volt)	30	40	50
Tool inner diameter	I (μm)	200	250	300

Table 2. Fixed parameters.

Parameter	Value/type
Workpiece material	Stainless steel 304
Machining time	60 s
Tool diameter	0.8 mm
Tool federate	1 mm/min

3. Jet-ECM process simulation

ECM is a chemical dissolution process in which a workpiece (anode) and a tool (cathode) are placed inside an electrolyte cell. A small voltage (V) is applied between the electrodes, and the tool moves toward the workpiece to perform the machining process [1]. The fundamental relations governing this process are Faraday's law, the Laplace equation, and Ohm's law [1, 30]. Faraday's law can be expressed as Eq. (1):

$$m = \frac{AIt}{zF}. \quad (1)$$

In the above relation, m represents the dissolved material machined with current (I) in time (t). A is the atomic weight, and z is the capacity of the material. A/z is the chemical equivalent, and F is the Faraday constant [1,30]. The basic equation in the electrochemical machining process is the Laplace equation, which is expressed as Eq. (2):

$$\nabla^2 \varphi = 0. \quad (2)$$

Eq. (2) describes the machining gap in the electrochemical machining process. By solving this equation, the potential (φ) at each node in the electrolyte (machining gap), especially at the workpiece surface, can be obtained using numerical methods. When the potential is established in the machining gap, a current is generated, and machining occurs. The current can be described by Ohm's law in this process [1,30]:

$$i = -k\nabla\varphi. \quad (3)$$

In Eq. (3), i represents the current density, and k is the electrical conductivity of the electrolyte.

This section aims to create a model, establish conditions, and simulate the Jet-ECM process using the COMSOL software. A two-dimensional symmetric model was employed. As shown in Figure 1, simulations were performed, and the boundary for the workpiece movement

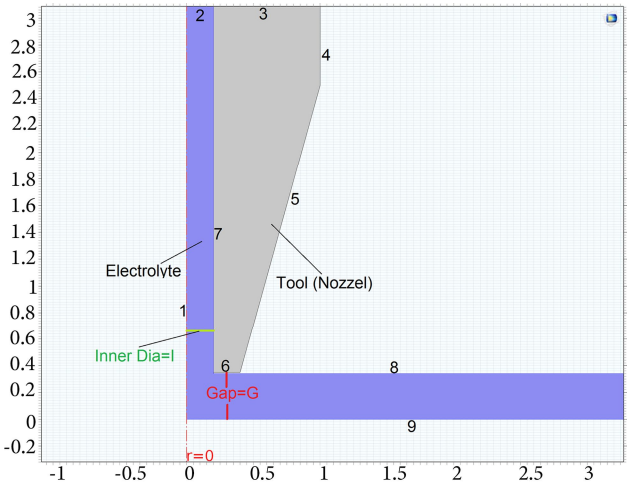

Figure 1. Geometry used for the two-dimensional symmetric analysis of Jet-ECM.

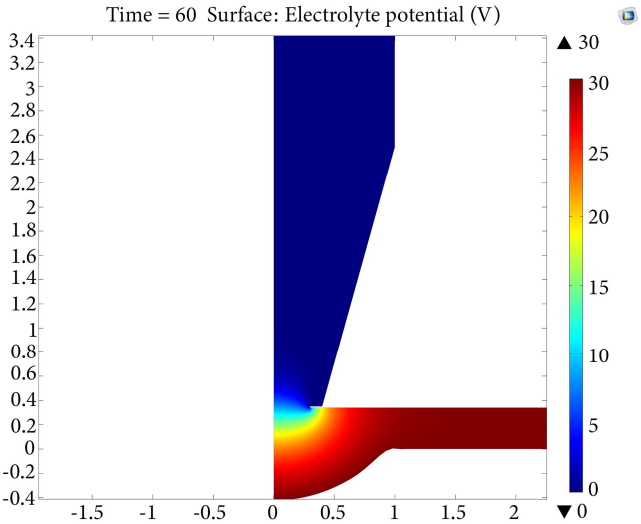

Figure 2. Electrolyte potential distribution in the electrolyte.

Table 3. Boundary conditions.

Boundary	Condition
1	Symmetry axis
2, 8	The potential gradient is zero
3-7	Tool boundary (Voltage=0)
9	Workpiece boundary (Machining voltage)

was obtained. Boundary conditions were considered for the process, as depicted in Figure 1 and summarized in Table 3 [30]. The potential gradient ($\nabla\phi$) is zero at the input and output of the electrolyte, the potential is zero at the tool's boundary, and the potential is equal to the machining voltage (V) at the workpiece's boundary. Triangular elements were utilized to create the mesh network.

The model was solved as a time-dependent variable for 60 seconds, and the results are presented in Figures 2 and 3. Figure 2 illustrates the potential distribution in the electrolyte, while Figure 3 depicts the change in the workpiece boundary over time.

4. Results and discussion

Table 4 presents the values related to the response variables for the 27 numerical simulations. As shown in Figure 3, the

Table 4. The values of response variables.

Run Order	Input parameters				Responses	
	C	V	G	I	D (mm)	E (mm)
1	12	40	200	200	0.530	0.130
2	8	50	350	250	0.415	0.120
3	12	40	200	300	0.618	0.270
4	12	40	350	250	0.455	0.192
5	8	40	200	250	0.475	0.040
6	12	40	500	300	0.395	0.260
7	8	40	350	300	0.395	0.108
8	12	30	350	300	0.425	0.168
9	16	40	200	250	0.658	0.293
10	12	40	350	250	0.455	0.192
11	12	50	500	250	0.404	0.268
12	12	30	200	250	0.503	0.099
13	12	50	350	300	0.558	0.374
14	12	40	350	250	0.455	0.192
15	16	40	500	250	0.425	0.278
16	16	30	350	250	0.454	0.190
17	12	30	500	250	0.288	0.039
18	16	40	350	300	0.575	0.390
19	8	30	350	250	0.293	0.090
20	12	40	500	200	0.303	0.036
21	16	40	350	200	0.475	0.205
22	12	30	350	200	0.342	0.018
23	8	40	350	200	0.312	0.070
24	8	40	500	250	0.250	0.030
25	12	50	200	250	0.639	0.288
26	16	50	350	250	0.595	0.400
27	12	50	350	200	0.455	0.188

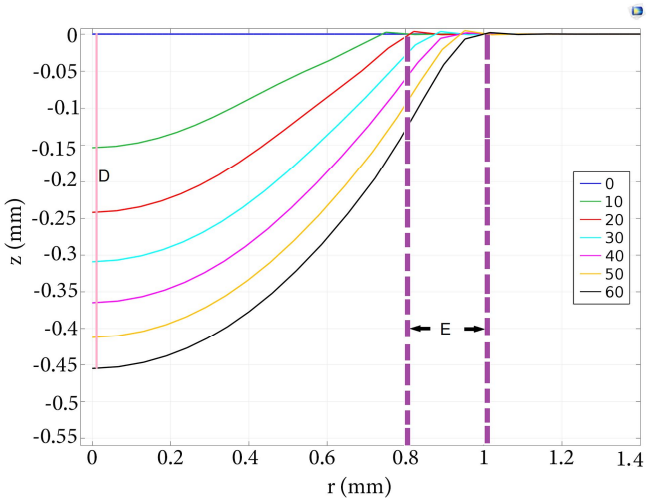

Figure 3. Deformation of the workpiece boundary.

depth of machining, indicated by D, is equal to the maximum displacement of the workpiece along the Z-axis after one minute. The hole is expected to be 0.8 mm in diameter. Deviations from this value are considered dimensional accuracy, denoted by E, as shown in the figure. The validation of the numerical simulation with practical experiments has been reviewed in another study [31].

4.1. Mathematical modeling of the depth of machining using RSM

The results of the Analysis of Variance (ANOVA) related to the machining depth (D) are presented in Table 5. The quadratic mathematical model in terms of un-coded input parameters is as follows:

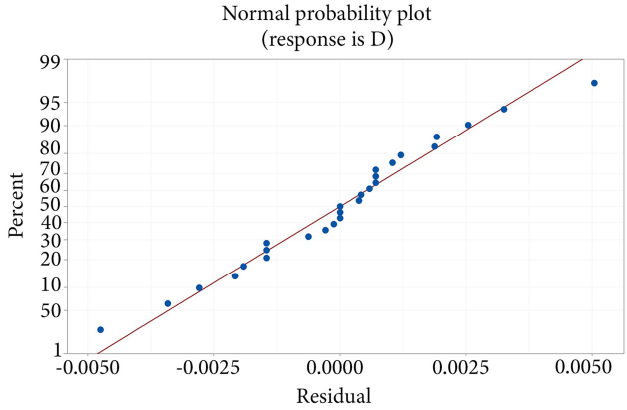

Figure 4. Normal probability plot for depth of machining (D).

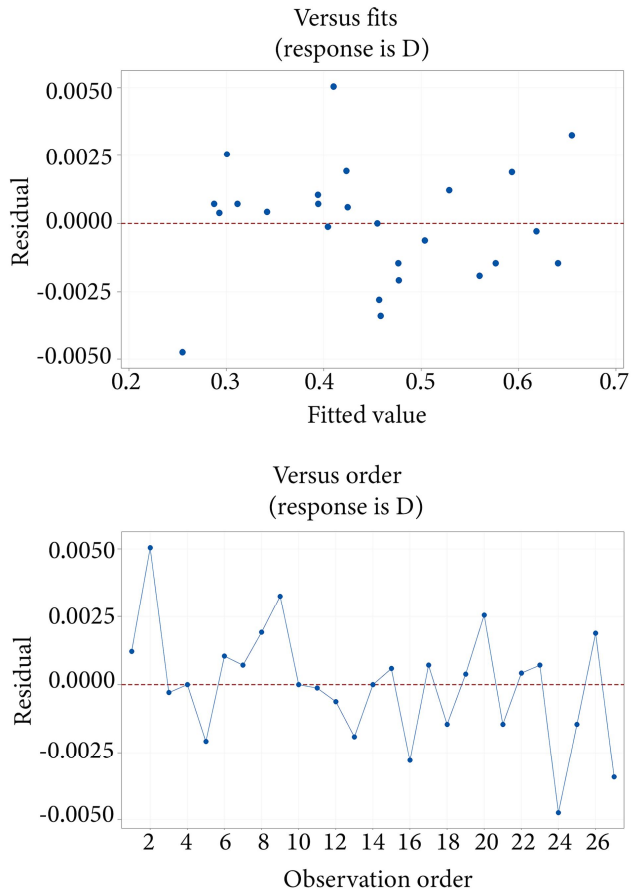

Figure 5. Residual diagram for depth of machining (D).

$$D = -0.0881 + 0.03006C + 0.00788V - 0.000902G + 0.000988I - 0.000719C * C - 0.000054V * V - 0.000002I * I + 0.000119C * V - 0.000003C * G + 0.000021C * I - 0.000003V * G + 0.000010V * I. \quad (4)$$

According to the ANOVA, the p-value for the quadratic model is significantly less than 0.05, indicating the adequacy of the model within a 95% confidence interval. Additionally, the values of correlation coefficients R^2 and R^2adj for the model are 99.97% and 99.92%, respectively.

Figure 4 shows a close correlation between the simulation and estimated values for the response variable. The residual diagram in Figure 5 has also been examined, and no pattern is observed, indicating the model's adequacy.

Table 5. ANOVA for machining depth.

Source	DF	Adj SS	Adj MS	*F*-value	*p*-value
Model	14	0.319837	0.022846	2464.24	0.000
Linear	4	0.317537	0.079384	8562.81	0.000
C	1	0.090480	0.090480	9759.68	0.000
V	1	0.048260	0.048260	5205.58	0.000
G	1	0.153680	0.153680	16576.76	0.000
I	1	0.025117	0.025117	2709.22	0.000
Square	4	0.001917	0.000479	51.71	0.000
C*C	1	0.000705	0.000705	76.08	0.000
V*V	1	0.000154	0.000154	16.62	0.002
G*G	1	0.000456	0.000456	49.22	0.000
I*I	1	0.000080	0.000080	8.64	0.012
2-Way interaction	6	0.000382	0.000064	6.88	0.002
C*V	1	0.000090	0.000090	9.73	0.009
C*G	1	0.000016	0.000016	1.73	0.214
C*I	1	0.000072	0.000072	7.79	0.016
V*G	1	0.000100	0.000100	10.79	0.007
V*I	1	0.000100	0.000100	10.79	0.007
G*I	1	0.000004	0.000004	0.43	0.524
Error	12	0.000111	0.000009		
Lack-of-fit	10	0.000111	0.000011	*	*
Pure error	2	0.000000	0.000000		
Total	26	0.319949			

R-sq=99.97%, **R-sq(adj)**=99.92%

4.2. Mathematical modeling of the dimensional accuracy using RSM

Similar to the previous section, the mathematical model of the dimensional accuracy (E) is obtained as Eq. (5), according to Table 6 for the analysis of variance:

$$E = 0.679 - 0.0620C - 0.0139V - 0.000323G - 0.00229I - 0.000047C * C + 0.000027V * V - 0.000001G * G - 0.001125C * V - 000002C * G + 0.000184C * I + 0.000007V * G + 0.000018V * I + 0.000003G * I. \quad (5)$$

Based on the ANOVA results, the p-value for the model is much less than 0.05, which is desirable. Furthermore, the values of correlation coefficients R^2 and R^2adj for this model are 96.82% and 93.11%, respectively. The normal and residual diagrams in Figures 6 and 7 demonstrate the adequacy and accuracy of the model.

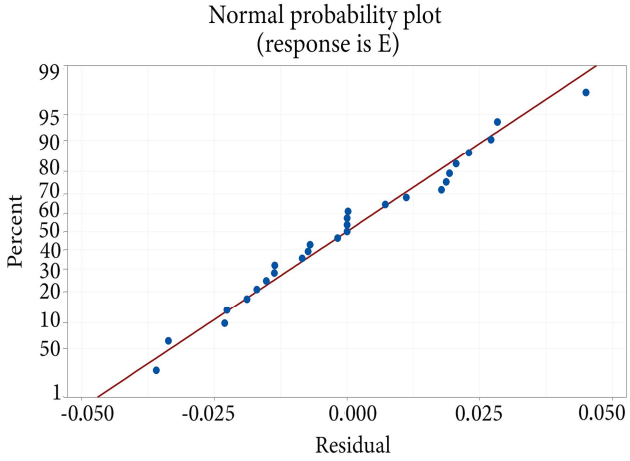

Figure 6. Normal probability plot for dimensional accuracy (E).

4.3. Investigation of the effect of input parameters on the responses

Referring to Table 5, the linear terms of the model for the depth of machining have the most significant impact on this response. The quadratic terms of the model and the interaction between the voltage (V) and the other three parameters are also significant. Additionally, Figure 8(a) indicates that increasing the conductivity (C) of the electrolyte, voltage (V), and inner diameter (I) of the tool leads to an increase in the depth of machining. Decreasing the initial machining gap (G) also increases the machining depth. Higher levels of these three parameters increase the current in the machining gap, consequently enhancing the dissolution rate.

According to Table 6, for dimensional accuracy, the linear terms of the model are significant. The p-value and F-value obtained from the analysis of variance indicate that the conductivity of the electrolyte (C), voltage (V), and internal diameter (I) of the nozzle have the most significant effect on the dimensional accuracy, respectively. Moreover,

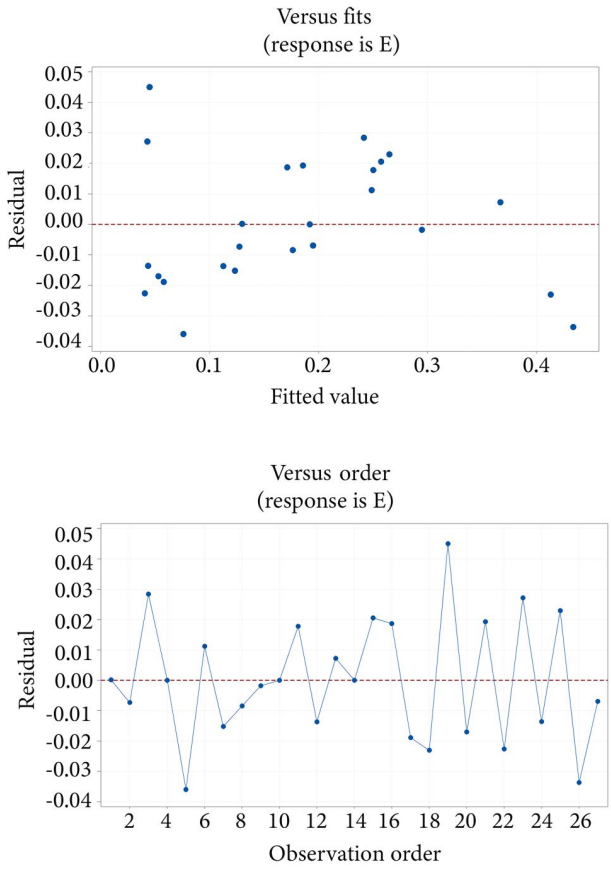

Figure 7. Residual diagram for dimensional accuracy (E).

the interaction between the conductivity of the electrolyte (C), voltage (V), and inner diameter (I) of the nozzle is also significant. As shown in Figure 8(b), lower levels of voltage (V), electrolyte conductivity (C), and nozzle diameter (I) improve the dimensional accuracy. By reducing these three parameters, the current density is focused on the machined gap, resulting in reduced stray currents during the process and improved accuracy.

4.4. Optimization with the desirability approach

In the desirability function approach, the goal is to determine the values of the input variables so that all the responses have a desirability greater than zero. Moreover, the overall desirability is maximized [32,33]. The optimization goal in this study is to maximize the machining depth to achieve a dimensional accuracy of 0.05 mm.

The result obtained using the Minitab software is presented in Figure 9. In this figure, the first row represents the input parameters and the range of their changes. The parameter's optimal value is between the variable's upper and lower limits. Each cell in the figure describes how the response variable changes concerning the change of one parameter while the other parameters are constant. Also, the red vertical line in each cell represents the value of the optimal input parameter, and the blue dashed line represents the value of the optimal response variable.

Therefore, the machining depth is optimized to achieve the desired dimensional accuracy of 0.05 mm, as presented in Figure 9. The conductivity of the electrolyte is 8 S/m, the voltage is 36.9 V, the initial machining gap is 200 µm, and the inner tool diameter is 0.4 mm, which has been determined as the optimal value for the optimization results.

5. Conclusion

The proposed approach, a combination of the numerical method

Table 6. ANOVA for dimensional accuracy.

Source	DF	Adj SS	Adj MS	*F*-value	*p*-value
Model	14	0.323994	0.023142	26.14	0.000
Linear	4	0.304131	0.076033	85.89	0.000
C	1	0.140400	0.140400	158.60	0.000
V	1	0.089096	0.089096	100.65	0.000
G	1	0.003640	0.003640	4.11	0.065
I	1	0.070994	0.070994	80.20	0.000
Square	4	0.003867	0.000967	1.09	0.404
C*C	1	0.000002	0.000002	0.00	0.965
V*V	1	0.000045	0.000045	0.05	0.825
G*G	1	0.002935	0.002935	3.32	0.094
I*I	1	0.000000	0.000000	0.00	0.987
2-Way interaction	6	0.015997	0.002666	3.01	0.049
C*V	1	0.008100	0.008100	9.15	0.011
C*G	1	0.000006	0.000006	0.01	0.934
C*I	1	0.005402	0.005402	6.10	0.029
V*G	1	0.000400	0.000400	0.45	0.514
V*I	1	0.000324	0.000324	0.37	0.556
G*I	1	0.001764	0.001764	1.99	0.183
Error	12	0.010623	0.000885		
Lack-of-fit	10	0.010623	0.001062	*	*
Pure error	2	0.000000	0.000000		
Total	26	0.334617			

R-sq=96.83%, **R-sq(adj)**= 93.12%

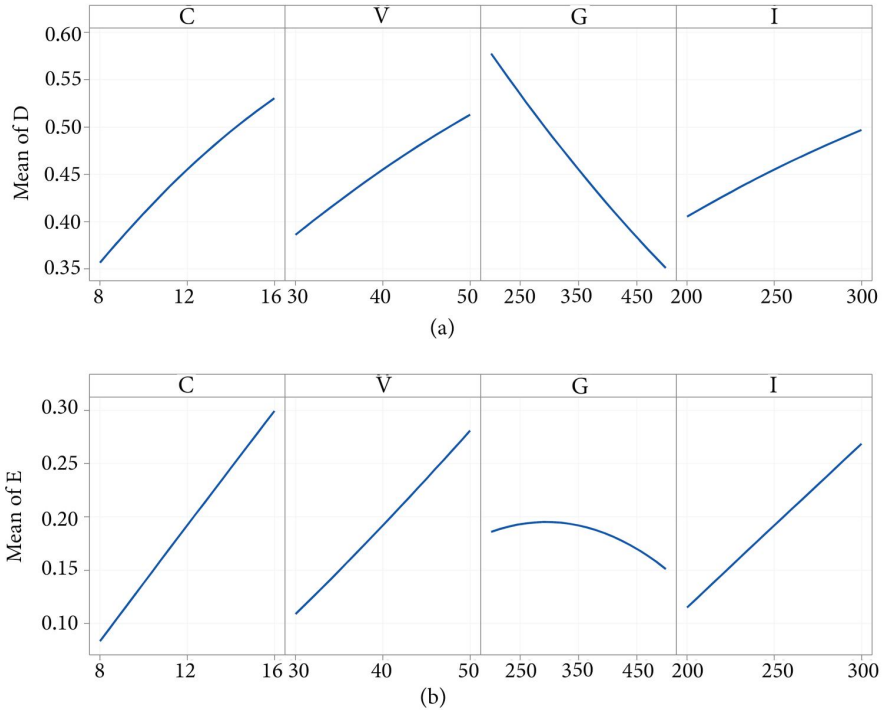

Figure 8. The effect of input parameters on (a) depth of machining and (b) dimensional accuracy.

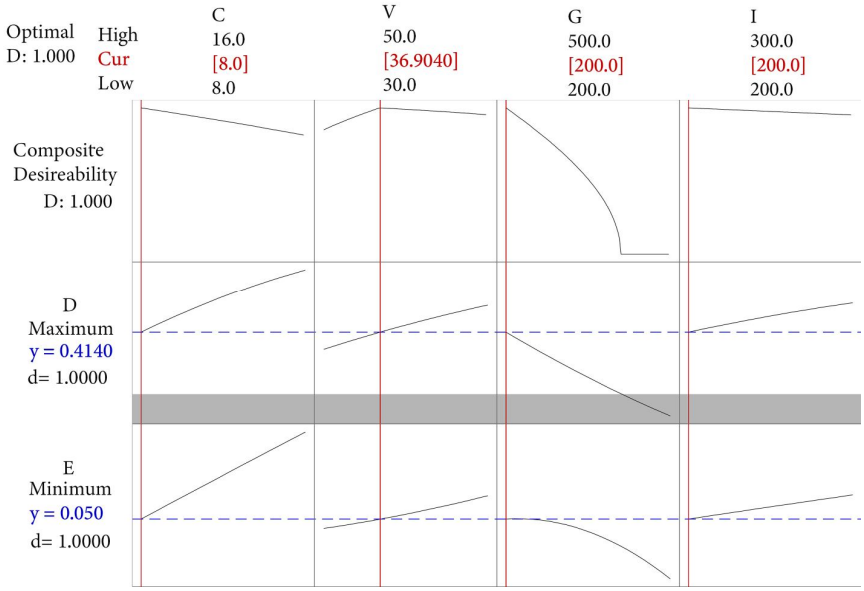

Figure 9. Optimization results for achieving the maximum machining depth at a dimensional accuracy of 0.05 mm.

method and the Design of Experiment (DOE) method, can be used for problems where access to materials is limited, or the experiments are costly and impractical. In this paper, with the help of this approach, modeling, and optimization of the Jet Electrochemical Machining (Jet-ECM) process have been performed. The following results are presented using this proposed approach:

- Mathematical models express the relationship between the input parameters of the Jet-ECM process (voltage, electrolyte conductivity, initial machining gap, and internal nozzle diameter) and response variables (depth of machining and dimensional accuracy) for 304 stainless steel;
- All the linear and quadratic terms and the interaction between voltage and the other three parameters are significant in machining depth;
- All the linear terms and the interaction of the electrolyte electrical conductivity with the voltage and the inner diameter of the nozzle are significant in the dimensional accuracy;
- Increasing the conductivity of the electrolyte, the voltage, and the inner diameter of the tool, as well as decreasing the initial machining gap, causes an increase in the machining depth;
- Low levels for the voltage, the electrolyte conductivity, and the internal nozzle diameter improve dimensional accuracy;
- The optimal values for achieving the maximum machining depth for a dimensional accuracy of 0.05 mm using the desirability function are electrolyte conductivity of 8 S/m, voltage of 36.9 V, initial machining gap of 200 μm, and inner tool diameter of 0.4 mm.

References

1. Rumyantsev, E. and Davydov, A. "Electrochemical machining of metals", MIR Publishers, Moscow (1989).

2. Mehrvar, A., Basti, A., and Jamali, A. "Inverse modelling of electrochemical machining process using a novel combination of soft computing methods", *P. I. Mech. Eng. C-J Mec.*, **234**, pp. 3436-3446 (2020). DOI: 10.1177/0954406220916495

3. Bergs, T. and Harst, S. "Development of a process signature for electrochemical machining", *CIRP. Ann-Manuf. Techn.,* **69**, pp. 153-156 (2020). DOI: 10.1016/j.cirp.2020.04.078

4. Leese, A. and Ivanov, A. "Electrochemical micromachining: Review of factors affecting the process applicability in micro-manufacturing", *P. I. Mech. Eng. B-J Manuf.*, **232**(2), pp. 195-207 (2017). DOI: 10.1177/0954405416640172

5. Kendall, T., Diver, C., Gillen, D., et al. "New insights on manipulating the material removal characteristics of jet-electrochemical machining through nozzle design", *Int. J. Adv. Manuf. Technol.*, **118**, pp. 1009-1026 (2022). DOI: 10.1007/s00170-021-07777-x

6. Hackert-Oschätzchen, M., Paul, R., Martin, A., et al. "Study on the dynamic generation of the jet shape in jet electrochemical machining" *J. Mater. Process. Tech.*, **223**, pp. 240-251 (2015). DOI: 10.1016/j.jmatprotec.2015.03.049

7. Kendall, T., Bartolo, P., Gillen, D., et al. "A review of physical experimental research in jet electrochemical machining", *Int. J. Adv. Manuf. Technol.*, **105**, pp. 651-667 (2019). DOI: 10.1007/s00170-019-04099-x

8. Niu, S., Qu, N., Fu, S., et al. "Investigation of inner-jet electrochemical milling of nickel-based alloy GH4169/Inconel 718", *Int. J. Adv. Manuf. Technol.*, **93**, pp. 2123–2132 (2017). DOI: 10.1007/s00170-017-0680-8

9. Wienand, T., Meichsner, G., and Hackert-Oschätzchen, M. "Jet electrochemical machining simulation of intersecting line removals with adjustable nozzle diameter by a finite area element grid", *Procedia CIRP.*, **102**, pp. 349-354 (2021). DOI: 10.1016/j.procir.2021.09.060

10. Ippolito, R., Tornincasa, S.G., Capello, C.R.F., et al. "Electron-jet drilling - Basic Involved Phenomena", *CIRP Annals.*, **30**(1), pp. 87-90 (1981). DOI: 10.1016/S0007-8506(07)60901-9

11. Speidel, A., Bisterov, I., Kumar Saxen, K., et al. "Electrochemical jet manufacturing technology: From fundamentals to application", *Int J Mach Tool Manu.*, **180**, pp. 103931 (2022).

    DOI: 10.1016/j.ijmachtools.2022.103931

12. Mehrvar, A., Basti, A., and Jamali, A. "Optimization of electrochemical machining process parameters: Combining response surface methodology and differential evolution algorithm", *P. I. Mech. Eng. E-J. Pro.*, **231**, pp. 1114-1126 (2017). DOI: 10.1177/0954408916656387

13. Venkata Rao, R. and Kalyankar V.D. "Optimization of modern machining processes using advanced optimization techniques: a review", *Int J Adv Manuf Technol.*, **73**, pp. 1159-1188 (2014). DOI: 10.1007/s00170-014-5894-4

14. Mukherjee, R. and Chakraborty, S. "Selection of the optimal electrochemical machining process parameters using biogeography-based optimization algorithm", *Int J Adv Manuf Technol.*, **64**, pp. 781-791 (2013). DOI: 10.1007/s00170-012-4060-0

15. Mehrvar, A., Motamedi, M., and Mirak, A. "Modeling of electrochemical machining of nickel-based single crystal super alloy by combining numerical and design of experiments methods", *Journal of Solid and Fluid Mechanics.*, **10**(3), pp. 207-217 (2020). DOI: 10.22044/JSFM.2020.9576.3162

16. Guo, C., Qian, J., and Reynaerts, D. "A three-dimensional FEM model of channel machining by scanning micro electrochemical flow cell and jet electrochemical machining", *Precis Eng.*, **52**, pp. 507-519 (2018). DOI: 10.1016/j.precisioneng.2018.02.002

17. Hackert-Oschätzchen, M., Paul, R., Kowalick, M., et al. "Multiphysics simulation of the material removal in Jet Electrochemical Machining", *Procedia CIRP.*, **31**, pp. 197-202 (2015). DOI: 10.1016/j.procir.2015.03.098

18. Paul, R., Hackert-Oschätzchen, M., Danilov, I., et al. "3D multiphysics simulation of jet electrochemical machining of intersecting line removals", *Procedia CIRP.*, **82**, pp. 196-201 (2019). DOI: 10.1016/j.procir.2019.04.154

19. Mitchell-Smith, J. and Clare, A.T. "Electrochemical jet machining of titanium: Overcoming passivation layers with ultrasonic assistance", *Procedia CIRP.*, **42**, pp. 379-383 (2016). DOI: 10.1016/j.procir.2016.02.215

20. Speidel, A., Sélo, R., Bisterov, I., et al. "Post processing of additively manufactured parts using electrochemical jet machining", *Mater Lett.*, **292**, pp. 129671 (2021). DOI: 10.1016/j.matlet.2021.129671

21. Liu, W., Kunieda, M., and Luo, Z. "Three-dimensional simulation and experimental investigation of electrolyte jet machining with the inclined nozzle", *J. Mater. Process. Tech.*, **297**, 117244 (2021).

    DOI: 10.1016/j.jmatprotec.2021.117244

22. Luo, J., Fang, X., and Zhu, D. "Jet electrochemical machining of multi-grooves by using tube electrodes in a row", *J. Mater. Process. Tech.*, **283**, 116705 (2020). DOI: 10.1016/j.jmatprotec.2020.116705

23. Hackert-Oschätzchen, M., Paul, R., Martin, A., et al. "Study on the dynamic generation of the jet shape in jet

electrochemical machining", *J. Mater. Process. Tech.*, **223**, pp. 240–251 (2015).

DOI: 10.1016/j.jmatprotec.2015.03.049

24. Chen, X., Zhu, J., Xu, Z., et al. "Modeling and experimental research on the evolution process of micro through-slit array generated with masked jet electrochemical machining", *J. Mater. Process. Tech.*, **298**, 117304 (2021). DOI: 10.1016/j.jmatprotec.2021.117304

25. Hackert-Oschätzchen, M., Martin, A., Meichsner, G., et al. "Microstructuring of carbide metals applying jet electrochemical machining", *Precis Eng.*, **37**(3), pp. 621–634 (2013). DOI: 10.1016/j.precisioneng.2013.01.007

26. Hung, J.C., Liu, J.H., and Fan, Z.W. "Fabrication of microscale concave and grooves through mixed-gas electrochemical jet machining", *Precis Eng.*, **55**, pp. 310–321 (2019). DOI: 10.1016/j.precisioneng.2018.09.020

27. Chen, X.L., Dong, B.Y., Zhang, C.Y., et al. "Jet electrochemical machining of micro dimples with conductive mask", *J. Mater. Process. Tech.*, **257**, pp. 101–111 (2018). DOI: 10.1016/j.jmatprotec.2018.02.035

28. Zhang, X., Song, X., Ming, P., et al. "The effect of electrolytic jet orientation on machining characteristics in jet electrochemical machining", *Micromachines.*, **10**(6), 404 (2019). DOI: 10.3390/mi10060404

29. Myers, R.H. and Montgomery, D.C., *Response Surface Methodology: Process and Product Optimization Using Designed Experiments*, Wiley, New York (1995).

30. Sun, C., Zhu, D., Li, Z., et al. "Application of FEM to tool design for electrochemical machining freeform surface", *Finite Elem Anal Des.*, **43**(2), pp. 168–172 (2006). DOI: 10.1016/j.finel.2006.08.004

31. Mehrvar, A., Mirak, A., and Rezaei, M. "Numerical and experimental investigation of electrochemical machining of nickel-based single crystal superalloy", *Modares Mech Eng.*, **20**, pp. 1873–1881 (2020).

32. Assarzadeh, S. and Ghoreishi, M. "A dual response surface-desirability approach to process modelling and optimization of Al_2O_3 powder-mixed electrical discharge machining (PMEDM) parameters", *Int J Adv Manuf Technol.*, **64**, pp. 1459–1477 (2013). DOI: 10.1007/s00170-012-4115-2

33. Mehrvar, A., Basti, A., and Jamali, A. "Modeling and parameter optimization in electrochemical machining process application of dual response surface desirability approach", *Lat Am Appl Res.*, **47**(4), pp. 157–162 (2017). DOI: 10.52292/j.laar.2017.317

Biographies

Ali Mehrvar is an Assistant Professor of Mechanical Engineering at University of Isfahan, Shahreza Campus, Iran. He received his PhD, MSc and BSc degrees in Manufacturing Engineering from University of Guilan, K.N. Toosi University of Technology and Isfahan University of Technology, Iran, respectively. His main research interests include non-traditional machining, micro and nano manufacturing processes, optimization and numerical analysis.

Mohsen Motamedi is an Assistant Professor of Mechanical Engineering at University of Isfahan, Shahreza Campus, Iran. He received his PhD and MSc degrees in mechanical engineering from University of Tehran (2015). His research interests include nano-mechanics, finite-element method, molecular dynamics simulation, composite and nano-composite materials, and fracture mechanics. He also has research activities in the field of modern manufacturing processes for new materials and superalloys.

Abouzar Jamalpour received his BSc degree in mechanical engineering from University of Isfahan, Shahreza Campus, Iran. He is a researcher at Isfahan Science and Technology Town (ISTT). His main activities are in machining processes and CNC programming. His main research interests include modern manufacturing processes and finite element methods.